

Article

Effect of CdSTe QDs' Crystal Size on Viability and Cytochrome P450 Activity of CHO-K1 and HEP-G2 Cells

Luis Alamo-Nole , Adriana Ponton-Almodovar and Ivan Ortiz-Laboy

Natural Sciences Department, Pontifical Catholic University of Puerto Rico, Ponce, PR 00717, USA

* Correspondence: luis_alamo@pucr.edu

Abstract: In the last few years, quantum dots (QDs) have attracted research interest in different fields of science and technology. Despite their applications, it is essential to understand how nanomaterials (with different crystal sizes) are metabolized inside organisms. Thus, the focus of this study was on an evaluation of how crystal sizes of CdSTe QDs affect the viability and response of the cytochrome P450 system in CHO-K1 and HEP-G2 cells. CdSTe QDs were synthesized using a microwave-assisted system at different reaction temperatures (60, 120, 150, and 180 °C) to obtain different crystal sizes. The optical and structural characterization confirmed four crystal sizes from 3 to 8 nm. Fluorescence microscopy confirmed that CdSTe QDs are incorporated into both cell lines. Viability studies suggested that CHO-K1 cells are more sensitive than HEP-G2 cells to CdSTe QDs and Cd⁺² ions. The responsible mechanisms for the toxicity of QDs and Cd⁺² are apoptosis followed by necrosis. The activity of CYP 1A1, 1A2, and 3A4 isoenzymes suggests that the smallest CdSTe crystals are recognized in a manner similar to that of Cd⁺². Furthermore, the largest CdSTe crystals can have different metabolic routes than Cd⁺².

Keywords: CdSTe QDs; crystal size; viability; cytochrome P450; nanotoxicity; HEP-G2 cells; CHO-K1 cells



Citation: Alamo-Nole, L.; Ponton-Almodovar, A.; Ortiz-Laboy, I. Effect of CdSTe QDs' Crystal Size on Viability and Cytochrome P450 Activity of CHO-K1 and HEP-G2 Cells. *Micro* **2023**, *3*, 308–319. <https://doi.org/10.3390/micro3010021>

Academic Editor: Ajit Roy

Received: 19 January 2023

Revised: 7 February 2023

Accepted: 24 February 2023

Published: 2 March 2023



Copyright: © 2023 by the authors. Licensee MDPI, Basel, Switzerland. This article is an open access article distributed under the terms and conditions of the Creative Commons Attribution (CC BY) license (<https://creativecommons.org/licenses/by/4.0/>).

1. Introduction

Nanoparticles (NPs) are classified according to their morphology, size, and chemical properties. For example, quantum dots (QDs) are semiconductor NPs ranging from 1 to 10 nm that can be synthesized in an aqueous medium by microwave systems [1,2]. The most significant properties of QDs are particle surface activation and a high surface area. As a result, QDs exhibit different physical, chemical, and biological properties than the corresponding bulk solid material. In addition, the small particle size of QDs leads to unique features regarding their electromagnetic, morphological/structural, optical, and thermal properties [3].

The concentrations of quantum dots (QDs) in the vicinity of municipal or industrial wastewater have increased due to material fabrication, transport, handling, usage, and waste disposal, which has exposed organisms and the environment to these particles [4,5]. In addition, engineered nanoparticles contaminate the environment through the discharge of wastewater [6,7]. As a result, approximately 10.3 megatons/year of nanomaterials are released into the environment [8].

Cadmium-based QDs can be synthesized using organometallic routes, colloidal precipitation, direct injection, and green chemistry methods. The microwave-assisted method is considered a green methodology that allows for the control of crystal sizes based on the reaction temperature. It uses low-toxicity reagents and produces water-stable QDs. CdSTe QDs synthesized via this method have shown excellent optical properties and water stability [9]. Although shelled QDs are environmentally stable and possess low metal release properties, they have low water stability due to their larger crystal size.

Due to their small size, QDs can easily enter organisms, which mainly occurs through endocytosis [10]. Once inside, they can interact with the microenvironment around the

cells or the plasma membrane [10,11]. Therefore, the viability of different cell lines exposed to various QDs is constantly studied.

Although the effects of cadmium ions have been studied, the cell responses to Cd-based QDs such as CdO [12], CdS [13], and CdSe [14] are still being researched. Cadmium-based QDs can produce reactive oxygen species (ROS) during their excitation and relaxation states. In addition, the exposure of Cd-based QDs to oxidative environments or low pH levels can cause the decomposition and leakage of cadmium (Cd^{2+}) ions, and this element is a toxic transition metal that is poorly excreted. ROS generated by the QDs and Cd ions in the body induce oxidative stress. ROS can destroy organelles and damage/hinder macromolecules, apoptosis, lipid peroxidation, mutagenesis, and cell death [15–17].

Chinese hamster ovary (CHO) cells are mammalian epithelial cells commonly used as a model for biological, medical, and pharmaceutical research. Due to their small size, low chromosome number, low cost, and rapid growth, they can synthesize proteins like human cells [18]. In addition, hepatoma cell lines such as HepG2 cells are used as alternative human hepatocytes. They have an epithelial-like morphology and allow for the study of drug metabolism and hepatotoxicity [19]. The responses of both cells are interesting, for instance, CHO cells are susceptible to drugs. Alternatively, HEP-G2 cells are less sensitive because they have more metabolic enzymes that allow for a more efficient degradation of drugs.

QDs can be considered xenobiotic substances that are foreign chemicals of a living system. In organisms, xenobiotics undergo biotransformation. For example, lipophilic xenobiotics are converted to hydrophilic metabolites to be eliminated. Cytochrome P450 (CYP), which is widely distributed throughout organisms, is the major enzymatic catalyst involved in the oxidation of xenobiotics [20]. CYP is a superfamily of heme-thiolate enzymes involved in the metabolism of exogenous compounds, including drugs, carcinogens, pesticides, heavy metals, and other pollutants. Various reactions catalyze these compounds, and the most common is oxidation by NADPH [20,21].

This research aims to evaluate if the CYP system recognizes CdSTe QDs as xenobiotics and how crystal size affects the viability and response of the CYP system in CHO-K1 and HEP-G2 cells.

2. Materials and Methods

2.1. Microwave-Assisted Synthesis and Characterization of CdSTe QDs

CdSTe QDs were synthesized by mixing deionized water and thioglycolic acid (TGA). TGA was used as a sulfur source and a complexing, stabilizing, and capping agent. In an alkaline environment, a cadmium precursor was added ($\text{CdSO}_4 \cdot 8/3\text{H}_2\text{O}$ solution), and a sodium hydrogen telluride (NaHTe) solution was used as the tellurium precursor. The NaHTe solution was prepared by reducing tellurium powder with NaBH_4 in a nitrogen-filled Scienceware portable glove box (Cole-Palmer, Vernon Hills, IL, USA) to avoid tellurium oxidation. The solution was transferred to a Teflon vessel and placed inside a MARS 6 microwave digestion system (CEM Corporation, Matthews, NC, USA). The reaction temperature was set at 60, 120, 150, or 180 °C for 15 min to obtain different crystal sizes. The CdSTe QDs were precipitated with 2-propanol, centrifuged, and dispersed in deionized water [9].

CdSTe QDs were characterized optically using an ultraviolet–visible (UV–Vis) 1800 spectrophotometer (Shimadzu, Columbia, MD, USA) and photoluminescence spectrofluorometer RF 6000 (Shimadzu, Columbia, MD, USA), and structurally by a D5000 X-ray diffractometer (Siemens, Aubrey, TX, USA) and high-resolution transmission electron microscopy JEM-ARM200CF (JEOL).

2.2. Cell Culture

The cell lines used in the study were the CHO-K1 (ATCC[®] CCL-61[™]) and HEP-G2 (ATCC[®] HBO-8065[™]) cell lines. CHO-K1 cells were cultured in F-12K medium and HEP-G2 were cultured in EMEM, which were supplemented with 10% fetal bovine serum (FBS)

and gentamycin. The cell cultures were maintained at 37 °C with 5% CO₂ in a Forma Steri-Cycle incubator (Thermo Fisher Scientific, Waltham, MA, USA).

2.3. Fluorescence Microscopy

The cells were detached by trypsinization. Glass coverslips were seeded and placed with cells inside Petri dishes. After incubation for 1 h at 37 °C, media were added to cover each coverslip and incubated at 37 °C for 24 h to allow cells to adhere to the coverslips. Following incubation, each medium was substituted with fresh medium and 10 mg/L of QDs. The Petri dishes were incubated for 2 to 4 h, which allowed the QDs to enter the cells. The medium was removed, and 4% p-formaldehyde was added to fix the cells. The cells were incubated at 4 °C for 20 min. The cells were washed three times with PBS. The coverslips were mounted and analyzed using a BX43 microscope with fluorescence (Olympus, Tokyo, Japan) at 10× and 40×.

2.4. Cell Viability Using Trypan Blue Exclusion Assay

After trypsinization, CHO-K1 and HEP-G2 cells were seeded in triplicate (1.0×10^4 to 1.0×10^5 cells/mL) into 24-well plates and incubated at 37 °C for 24 and 48 h, respectively, to allow the cells to attach to the plates. Next, the media were replaced with fresh media and QDs at 0.01–10 mg/L concentrations. Finally, the 24-well plates were incubated at 37 °C for another 24 h before analysis with a Cellometer Auto T4 cell counter (Nexcelom Bioscience, Lawrence, MA, USA). A 1:1 mixture of the cell suspension and a 0.2% trypan blue staining solution was used for the analysis.

2.5. CellTiter-Glo[®] Luminescent Cell Viability Assay

CHO-K1 and HEP-G2 cells were diluted to 10^4 cells/mL concentrations. The 96-well plates were prepared by adding 100 µL medium containing cells in five to six replicates. The plates were incubated at 37 °C for 24 and 48 h, respectively, to allow the cells to attach to the plates. The CdTe QDs and cadmium solution (0.001–10.0 mg/L) in culture media were then added and incubated for 24 to 48 h. The plates and their content were equilibrated at room temperature for 30 min, and 100 µL of the CellTiter-Glo[®] reagent (G7571 Promega, Madison, WI, USA) was added to each well. The contents were mixed for 2 min to induce cell lysis and incubated at room temperature for 10 min to stabilize the luminescent signal inside a Fluoroskan Ascent FL microplate luminometer (Thermo Fisher Scientific, Waltham, MA, USA).

A standard curve using CHO-K1 cells was plotted to confirm the kit's reliability using serial dilutions from 1.0×10^6 to 10 cells/mL. It also determined the suitable number of cells for the analysis. In addition, the cells were mixed with the CellTiter-Glo[®] reagent, and the luminescent signal was recorded. In addition, an ATP standard curve in 96-well plates was generated using 1.0, 100, and 10 nM of ATP in culture media and the same described protocol to confirm the linear relation between ATP and the kit reagents.

2.6. RealTime-Glo[™] MT Cell Viability Assay

The 96-well plates were prepared with CHO-K1 cells at a concentration of 10^4 cells/mL and incubated at 37 °C for 24 h (five to six replicates). The cells were mixed with QDs (0.001 to 10.0 mg/L) in fresh media and incubated for 24 h. Then, the RealTime-Glo[™] reagents were added and incubated for 1 h, and the luminescence was recorded.

For viability assays during 24 h, 96-well plates were prepared with 10^4 CHO-K1 cells/mL and incubated at 37 °C (five to six replicates). The cells were mixed with fresh media, QDs, and Real-time Glo[™] reagents (G9711 Promega, Madison, WI, USA). The plate was incubated, and the luminescence was recorded at specific times for 72 h. A standard curve was prepared using serial dilutions from 1.0×10^6 to 1.0×10^2 CHO-K1 cells/mL to confirm the reliability of the kit and the number of cells used in the experiments.

2.7. Apoptosis and Necrosis Assay

Cell death was evaluated using a RealTime-Glo™ Annexin V Apoptosis and Necrosis kit (JA1012 Promega, Madison, WI, USA). Apoptosis was monitored by exposing phosphatidylserine to the outer cell layer to release DNA and thus determine necrosis.

The 96-well plates were prepared with 50 µL of HEP-G2 cells (10^6 cells/mL), 50 µL of CdSte QDs, cadmium solution (5.0 mg/L) in medium, and 100 µL of the detection reagent. The plates were incubated at 37 °C, and the luminescence and fluorescence (485 nm of excitation and 525–530 nm of emission) were recorded at specific times for 72 h.

2.8. P450-Glo™ Assays

The Promega P450-Glo™ kits of CYP1A1 (Luciferin-CEE, V8752), CYP1A2 (Luciferin-1A2, V8422), CYP2B6 (Luciferin-2B6, V8322), CYP2C9 (Luciferin-H, V8792), and CYP3A4 (Luciferin-PFBE, V8902) were tested. The cytochrome P450 human enzymes provided by Sigma-Aldrich—CypExpress™ 1A1 (MTOXCE1A1-250MG), CypExpress™ 1A2 (MTOXCE1A2-250MG), CypExpress™ 2B6 (MTOXCE2B6-250MG), and CypExpress™ 2C9 (MTOXCE2C9-250MG)—were used to assure positive active results. Final concentrations of 1.25 mg/mL of each CYP enzyme and 6–100 µM of CYP substrates (suggested by the manufacturer) yielded good luminescence with relative standard deviations of about 10%. A critical difference that was determined with respect to the kit manufacturer was the reading time. The measurements were taken immediately after adding the luciferin detection reagent (with a 20 s agitation step at medium speed) instead of after 20 min of equilibration time. In addition, standard curves using kit reagents and D-luciferin were plotted to confirm the linear response.

The production of CYP enzymes in CHO-K1 cells was evaluated using different concentrations of substrates, exposure times, cell concentrations, QD concentrations, or integration times on a luminometer. However, the signal was too weak to obtain reproducible results. Therefore, all CYP isoenzyme experiments were performed with HEP-G2 cells at concentrations of about 3.0×10^6 cells.

HEP-G2 cells were seeded into opaque 96-well plates in five or six replicates and incubated at 37 °C for 48 h to allow cells to attach. The QDs (0.1, 1.0, 5.0, and 10.0 mg/L) and inductors (omeprazole and rifampicin) were added, and the plates were incubated at 37 °C for another 24 h to stimulate CYP isoenzyme production or inhibition. The culture media were replaced with fresh media containing the luminogenic CYP substrate for each enzyme. The plates were incubated at 37 °C for specific times based on each enzyme. The enzymes converted the luminogenic CYP substrate, a beetle luciferin derivative, to D-luciferin. An equal volume of luciferin detection reagent was added, and luminescence was recorded.

2.9. Statistical Analysis

A one-way ANOVA in the IBM SPSS statistical program was used to determine any statistically significant differences among the groups with a significance level of 0.95%. In addition, one-way ANOVA was used to determine differences among the control cells (0 mg/L) and the groups of cells exposed to different QD concentrations (and Cd⁺² ions) in the viability studies using the luminescent cell viability kit. In addition, it was also used to determine differences among the control cells (0 mg/L) and the response of CYP isoenzymes of cells exposed to different QD concentrations (and Cd⁺² ions) using the P450-Glo™ kits (Promega, Madison, WI, USA).

3. Results and Discussion

3.1. Synthesis and Characterization of CdSte QDs

During the synthesis, thioglycolic acid (TGA) allowed the production of CdSte QDs covered with TGA residues. Also, TGA avoided increasing crystal sizes and provided water stability. Figure 1a,b show the optical characterization by UV-Vis spectra and fluorescence of the CdSte QDs synthesized at different temperatures (60, 120, 150, and 180 °C). The spectrophotometry analysis shows a typical peak at about 380 nm (blue arrow) that was

used as the excitation wavelength in the fluorescence analysis. Shoulders related to the bandgap energy were observed at 505, 540, 570, and 630 nm (marked with sky-blue, yellow, green, and red arrows) for the QDs synthesized at 60, 120, 150, and 180 °C, respectively (Figure 1a). The fluorescence emission peaks (Figure 1b) correspond to the colors observed in the inserted Figure 1a (UV irradiated). These results confirmed that the changes in the optical properties were due to reaction temperature.

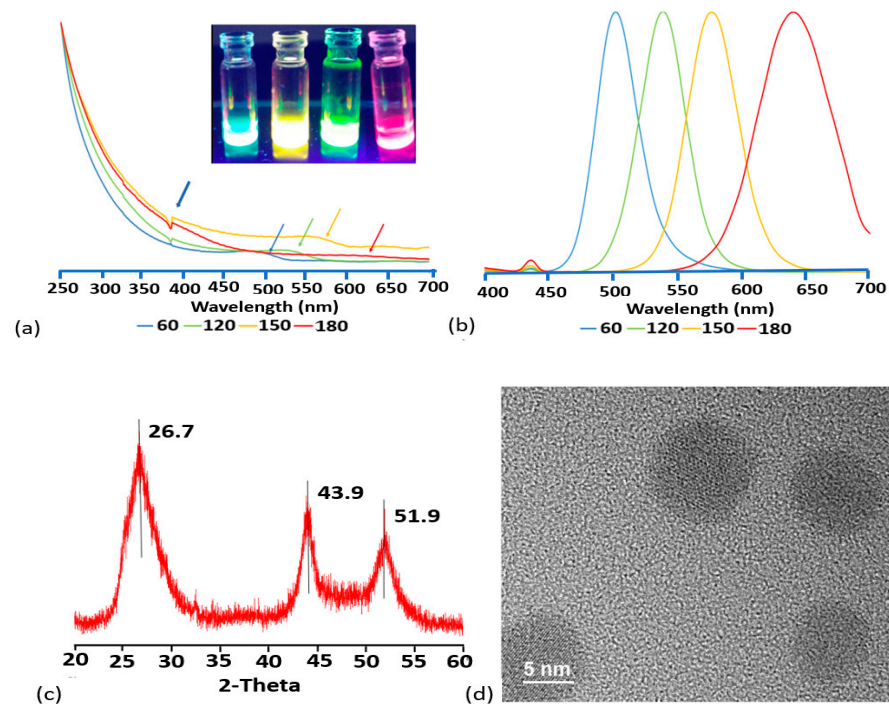


Figure 1. UV-Vis spectra (a), photoluminescence (b), XRD (c), and HR-TEM (d) analysis of CdSTe QDs. Sky-blue, yellow, green, and red arrows (a) denote the bandgap energy of each QD.

Figure 1c,d show the structural characterization of the CdSTe QDs by XRD and HR-TEM. The peaks at 26.5, 43.9, and 51.9° of the XRD spectra of the CdSTe QDs synthesized at 150 °C correspond to the planes 111, 220, and 311 of a cubic-blend zinc structure, and confirmed a solid solution of CdSTe. The HR-TEM spectra confirmed the nanometric size of the CdSTe QDs synthesized at 120 °C. All the CdSTe QDs have crystal sizes ranging from 3 to 8 nm.

3.2. Fluorescence Microscopy

The interactions of the CdSTe QDs and cells were examined by fluorescence microscopy with an excitation at 358 nm. All the CdSTe crystals absorbed the excitation wavelength, but the fluorescence was weak and impossible to observe for the QDs synthesized at 60 °C. Figure 2 shows HEP-G2 cells exposed to the CdSTe QDs synthesized at 120, 150, and 180 °C with characteristic green, yellow, and red fluorescence colors, respectively. In this figure, all the cells are non-extended and crowded. A slightly yellow emission with blue tones (lamp irradiation) can be observed. Figure 2 shows different fluorescence intensities, thus confirming the interaction and incorporation of the QDs inside the cells. After some hours of exposure to the QDs and ionic cadmium, the cells tended to detach from the coverslip, generating rounded cells. The nanomaterial affects the integrity of the membranes that are discussed below.

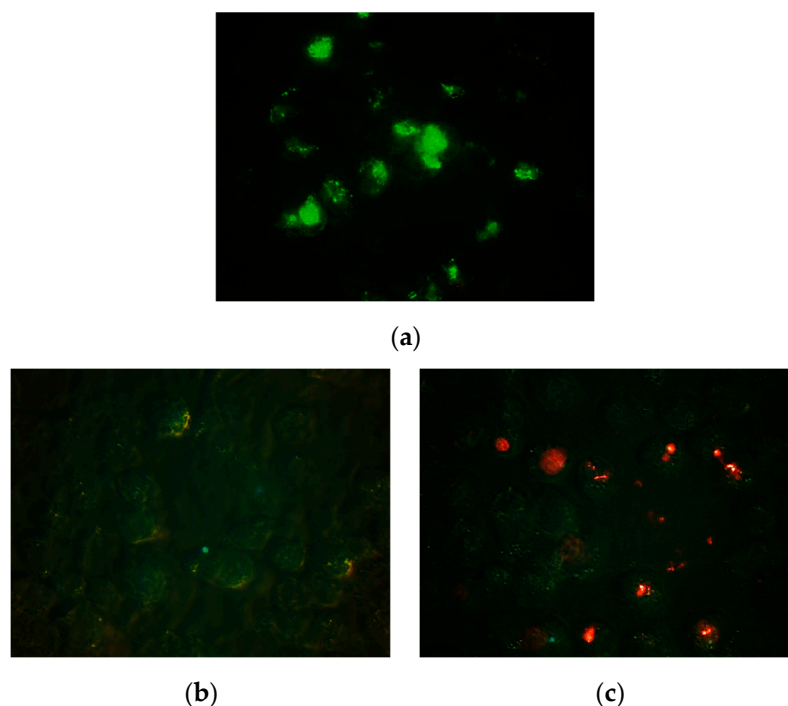


Figure 2. Fluorescence images of HEP-G2 cells exposed to CdSTe QDs synthesized at (a) 120 °C, (b) 150 °C, and (c) 180 °C (40×). Cells were exposed to 10 mg/L of each QD for 4 h at 37 °C and 5% CO₂ and fixed with p-formaldehyde. Excitation wavelength was 365 nm (50 nm) and emission was above 450 nm.

3.3. Viability Assays

The viability of the CHO cells was evaluated using three different assays (trypan blue exclusion, CellTiter-Glo[®] luminescent, and RealTime-Glo[™] MT assays) to select the one with the least variability. The CdSTe QDs synthesized at 60 and 120 °C were used. The trypan blue (TB) exclusion assay discriminates between viable and dead cells. Dead cells have a damaged membrane permeable to the TB dye, which stains the cytoplasm, producing a blue color under a microscope or when distinguished in a cell counter. The TB exclusion assay for cells exposed to the CdSTe QDs for 24 h suggested a slight decrease in cell viability (Table 1). The results indicated dose-dependent cytotoxicity. There was no difference in the viability between the QDs at concentrations of 1.0 and 10 mg/L.

Table 1. Viability of CHO-K1 cells determined using trypan blue, CellTiter-Glo[®] luminescent (AMP kit), and RealTime-Glo[™] MT (MT kit) assays exposed for 24 h to CdSTe QDs synthesized at 60 and 120 °C (concentrations between 0.01 and 10 mg/L).

Assay	Trypan Blue		AMP Kit		MT Kit	
	60	120	60	120	60	120
CdSTe QDs						
0	100 ± 6		100 ± 5		100 ± 10	
0.01			105 ± 6	83 ± 12	91 ± 8	93 ± 11
0.1	101 ± 2	102 ± 5	105 ± 5	87 ± 10	99 ± 14	101 ± 10
1.0	70 ± 9	69 ± 12	46 ± 1	38 ± 9	76 ± 17	67 ± 13
10	62 ± 7	66 ± 12	24 ± 3	18 ± 3	6 ± 2	14 ± 5

The CellTiter-Glo[®] luminescent cell viability kit (Promega G7570) is a lytic assay that detects ATP produced by metabolically active cells. The luminescent signal produced by a luciferase reaction and ATP is proportional to the ATP released after the lysis process.

The results also confirm that the cytotoxicity is dose-dependent. In addition, this kit detects differences among QDs synthesized at different temperatures and concentrations.

RealTime-Glo™ MT Cell Viability kit (Promega G9711) is a non-lytic assay that monitors a cell's viability over 72 h. The MT substrate is degraded intracellularly by active metabolic cells producing a compound that participates in a luminescent reaction (luciferase). We used the above kit to confirm the results of the CellTiter-Glo® luminescent cell viability kit. The results revealed dose-dependent cytotoxicity, differences among the QDs, and different concentrations. The slightly low variability (standard deviation) of the results obtained with the AMP kit was the foremost contributory factor leading to this kit's use in the following experiments.

The weak ability of the trypan blue assay to quantify the non-viable cells is explained in Figure 3. The figure shows how CHO-K1 and HEP-G2 cells are affected by the CdSTe QDs over time. The images are of the 96-well plates used in the viability assays and were captured using an inverted microscope. Immediately after the QDs were added, both cells presented characteristic long shapes, indicating that they were attached to the bottom of the plate. After the first 6 to 9 h, some cells were detached and assumed a quasi-spherical form. At 24 h, all the CHO-K1 cells and most HEP-G2 cells were detached and had assumed spherical shapes. The loss of morphology indicates affected or non-viable cells, so the production of ATP or the metabolism of the MT substrate was decreased. Cells have intact membranes; TB dye cannot enter cells, thereby generating false high viability. The same problems have been reported for this assay [22].

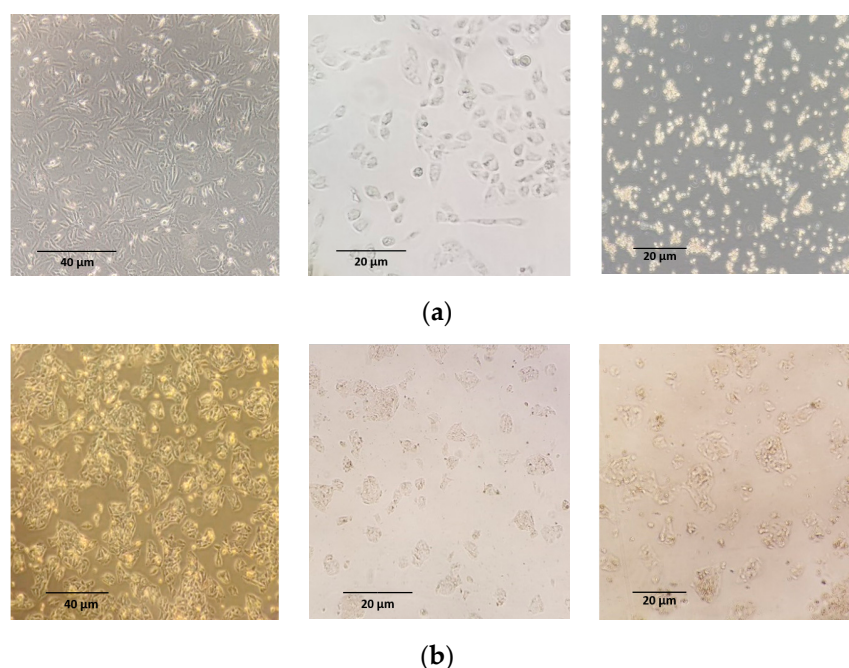


Figure 3. Microscopy images (via inverted microscope) of CHO-K1 cells (a) at 0 h (left), 6–9 h (center), and 24 h (right); HEP-G2 cells (b) at 0 h (left), 6–9 h (center), and 24 h (right) exposed to 10 mg/L CdSTe QDs.

Figure 4a,b show the viability of the CHO cells and HEP-G2 cells after 24 h of exposure to different crystal sizes (ranging between 3 and 8 nm) and cadmium ions (CdSO_4) at concentrations from 0.001 to 10 mg/L. Both cells present dose-dependent cytotoxicity. The same pattern has been observed for other Cd-based QDs [16]. There were no statistical differences in the viability based on the CdSTe crystal size for both cells and the same concentrations. Thus, although the optical and structural characterization confirmed changes in the crystal sizes from 3–8 nm, the surface area generated due to their sizes was insufficient to change the degree of viability. The greater capacity of the HEP-G2

cells to tolerate higher concentrations of Cd-QDs and cadmium ions than the CHO-K1 cells may be due to their ability to express cytochrome P450 isoenzymes. The expression of CYP enzymes in the CHO-K1 cells was evaluated by changing the concentrations of the substrates, the exposure times, the cell concentrations, the QD concentrations, or the integration time on the luminometer. In all the experiments, the expression level was too low (i.e., a very weak signal) to obtain reproducible results. This finding suggests that cells with low CYP expression (such as CHO cells) are more susceptible to cytotoxicity.

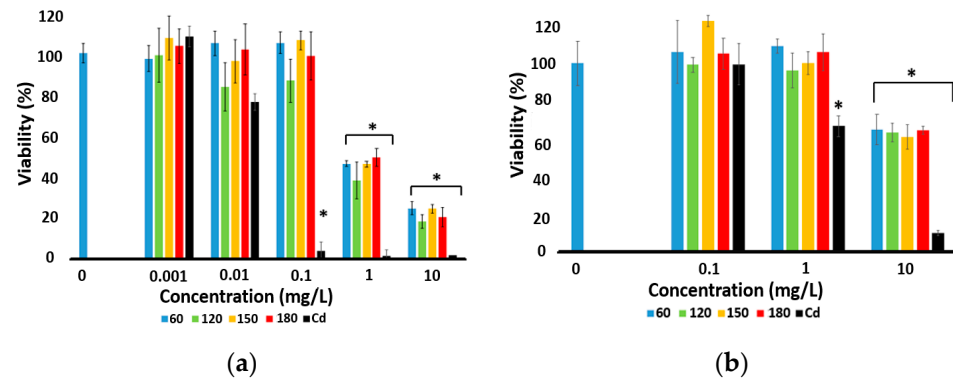


Figure 4. Viability (%) of CHO-K1 (a) and HEP-G2 (b) cells exposed to CdSTe QDs synthesized at different temperatures (60, 120, 150, and 180 °C) and cadmium solution at concentrations from 0.001 to 10 mg/L (CellTiter-Glo[®] luminescent cell viability assay) for 24 h. * statistical difference.

The TGA on the QDs' surfaces facilitates water stabilization and avoids the QDs' breakdown in the culture medium [23]. However, if QDs are accumulated for extended periods in cells that encounter acidic environments, TGA degradation and the oxidation of the QDs' cores may result [15,24]. When QDs enter cells, the pH values of the extracellular medium shift from 7.4 to 5.9–6.0 in early endosomes and to 5.0–5.5 within lysosomes [25]. The acidic conditions of these compartments can cause TGA's protonation and release from the surface and QDs' decomposition, resulting in the release of free Cd²⁺ ions [23]. These free Cd²⁺ ions can cause long-term toxicity.

The evident effect on the viability of both cells induced by the cadmium solution (Cd²⁺) at low concentrations suggests the action of a mechanism other than CdSTe QDs during the first hours of exposure. This pattern was confirmed by the apoptosis/necrosis and P450 assays discussed below.

The principal effect of QDs on living organisms is the production of reactive oxygen species (ROS) that can cause cell death. The photoexcitation of QDs promotes the transfer of an electron from the valence band to the conduction band, which creates an electron-hole pair. The electron or hole may interact with electron acceptors or donors, thus facilitating the generation of photoexcited QDs. ROS, such as superoxide anion (O₂⁻), hydrogen peroxide (H₂O₂), and hydroxyl radical (HO•), consist of radical and non-radical oxygen species. Oxidative stress produces direct or indirect ROS-mediated damage to nucleic acids, proteins, and lipids [26]. An ROS-Glo[™] H₂O₂ kit (Promega G8820) was used to quantify the production of H₂O₂ as an ROS indicator. The production of H₂O₂ was positively determined at high concentrations of CdSTe QDs (10 mg/L) in the media without cells. It was not possible to quantify H₂O₂ in the media with cells. Peroxidase enzymes rapidly deter H₂O₂ production [26].

3.4. Apoptosis and Necrosis Assay

Figure 5 suggests that the effects of the CdSTe QDs and Cd²⁺ ions are slightly different during the first hours of exposure. The shape of the curves for the QDs and Cd²⁺ confirms an apoptotic phenotype that leads to secondary necrosis (as suggested by the kit's manufacturer). There is a gap of 14 h and 22 h for the CdSTe QDs and Cd²⁺ ions, respectively, starting with an increase in the amount of apoptosis detected and leading

to an marked increase in necrosis. The shape of the curve for the blank cells indicates a non-apoptotic phenotype. The apoptosis generated by the Cd^{+2} ions starts at about 10 h and is the principal mechanism for cell viability loss at 24 h, as observed in Figure 4. The capacity of cadmium to produce apoptosis has been previously reported [27]. For CdSTe QDs, apoptosis starts at about 20 h due to the higher viability than Cd^{+2} . Although the degree of necrosis increases for the CdSTe QDs and Cd^{+2} ions, higher degrees of Cd^{+2} necrosis have been reported by other authors [28]. The detached and rounded cells shown in Figure 3 are an initial response to apoptosis.

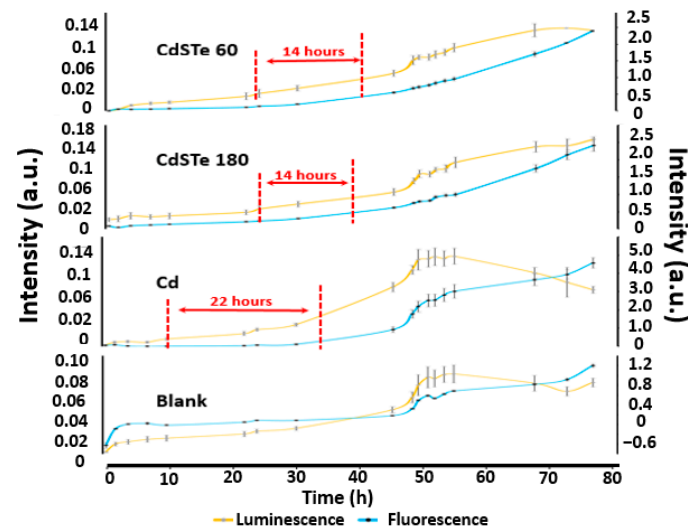


Figure 5. Luminescence and fluorescence indicate apoptosis and necrosis of HEP-G2 cells exposed to CdSTe QDs (synthesized at 60 and 180 °C at 2.0 mg/L) and cadmium solution at 2.0 mg/L. Fluorescence was recorded using 485 nm excitation and 525–530 nm emission.

3.5. The Activity of CYP450 Isoenzymes

Although we tested several CYP450 isoenzymes in the HEP-G2 cells, the 1A1, 1A2, and 3A4 isoenzymes (using Luciferin-CEE, Luciferin-1A2, and Luciferin PFBE as substrates, respectively) yielded the best results. In addition, the effect of metals on the CYP system has been observed [29–31].

Figure 6 shows the response of the (a) CYP 1A1, (b) CYP 1A2, and (c) CYP 3A4 isoenzymes of the HEP-G2 cells exposed to the CdSTe QDs and Cd^{+2} with and without inductors. The response of the cells (without CdSTe QDs, Cd^{+2} , or inductors) was set to 100%; values below this represent possible inhibition, and values above represent a potential induction.

There was isoenzyme activity detected for the CYP 1A1 isoenzyme (Figure 6a), but it did not change in the presence of the CdSTe QDs or Cd^{+2} . Instead, there was a marked response of the isoenzyme to the inductor, namely, a five-fold response. Similarly, the CYP 1A1 isoenzyme's response was not affected by the presence of the CdSTe QDs or Cd^{+2} . Thus, although some authors have reported that Cd^{+2} can induce a response from CYP1A and CYP2C9 isoenzymes [31], we did not obtain similar results using the Luciferin-CEE substrate.

For the CYP 1A2 isoenzyme (Figure 6b), although there were no statistical differences (except for CdSTe-150) in the activity without the inductor, we can observe some tendencies. The inductor generated a three-fold activity response. The CdSTe-60 QDs produced a slight decrease in activity without the inductor. Moreover, the marked activity reduction with the inductor indicates interferences with the capacity of this isoenzyme. These results have the same tendency as Cd^{+2} ; the small size of the QDs (high surface area) can generate a rapid degradation of the nanoparticle, releasing Cd^{+2} ions responsible for the toxicity and similar response [28–32]. Although there was a slight increase in the isoenzyme activity with

CdSTe-120 and CdSTe-150 without the inductor, the activity in the presence of the inductor did not change, suggesting there is no actual interference in the CYP 1A2 isoenzyme when using the luciferin-1A2 substrate.

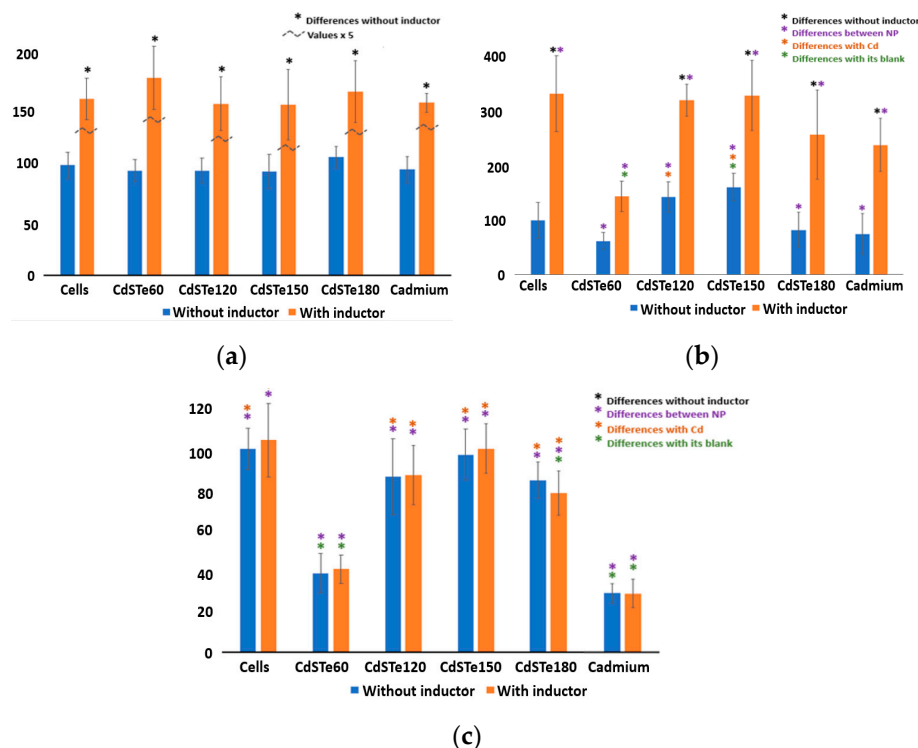


Figure 6. Responses of the (a) CYP 1A1, (b) CYP 1A2, and (c) CYP 3A4 isoenzymes to the HEP-G2 cells' exposure to CdSTe QDs and Cd²⁺ with and without an inductor (omeprazole or rifampicin) using Luciferin-CEE, Luciferin-1A2, and Luciferin-PFBE as substrates, respectively.

Regarding the CYP 3A4 isoenzyme (Figure 6c), the decrease in activity (with and without an inductor) using CdSTe-60 confirms its inhibition. The same results were obtained for the Cd²⁺ ions, which demonstrates that the smallest crystals can be recognized as xenobiotics, similar to cadmium ions. Although there was a slight decrease in the activity for CdSTe-180, in general, there were no changes in activity, indicating that for the larger crystals of the CdSTe QDs, the responses of some CYP450 isoenzymes are different from Cd²⁺ ions. Some authors suggest that the organic covers on the surface of nanoparticles can affect the response of metabolic enzymes [32].

4. Conclusions

It is essential to understand the possible metabolic routes of QDs for medical applications and their impacts on the environment. In this study, fluorescence microscopy confirmed that CdSTe QDs could enter CHO-K1 and HEP-G2 cells. Microscopy analysis suggested that CdSTe QDs generate small, rounded, non-viable cells after 24 h, which is in accordance with the apoptosis and necrosis results. CHO-K1 cells are more sensitive to CdSTe QDs and Cd²⁺ ions than HEP-G2, but the viability of both line cells is dose-dependent. CdSTe QDs are recognized as xenobiotics by HEP-G2 cells, thus generating changes in the CYP450 system. The smallest crystal size (CdSTe-60) inhibits the CYP1A2 and CYP3A4 isoenzymes, similar to Cd²⁺ ions. The differences in the responses of the CYP1A1 and CYP3A4 isoenzymes (with and without an inductor) of the HEP-G2 cells exposed to the largest crystals of the CdSTe QDs compared to Cd²⁺ ions suggest different metabolic processes inside the cells. Finally, cells that do not express CYP450 are more vulnerable to nanomaterials.

Author Contributions: Conceptualization, formal analysis, Funding acquisition, supervision, Writing—original draft, Writing—review and editing, L.A.-N.; Investigation, Methodology, A.P.-A. and I.O.-L. All authors have read and agreed to the published version of the manuscript.

Funding: The research reported in this publication was supported by an Institutional Development Award (IDeA) from the National Institute of General Medical Sciences of the National Institutes of Health under grant number P20 GM103475. The content is solely the authors' responsibility and does not necessarily represent the official views of the National Institutes of Health.

Institutional Review Board Statement: Not applicable.

Informed Consent Statement: Not applicable.

Data Availability Statement: The datasets generated during the current study are available from the corresponding author on reasonable request.

Acknowledgments: TEM work was performed at the National High Magnetic Field Laboratory, supported by National Science Foundation Cooperative Agreement No. DMR-1644779 and the State of Florida. The authors thank Monica Arroyo for editing the manuscript.

Conflicts of Interest: The authors declare no conflict of interest.

References

1. Li, J.; Zhou, X.; Ni, S.; Wang, X. One-pot synthesis of strongly luminescing CdTe quantum dots and their conjugation with mouse antibody to alpha-fetoprotein. *Colloid J.* **2010**, *72*, 710–715. [[CrossRef](#)]
2. Alamo-Nole, L.; Bailon-Ruiz, S.; Cruz-Acuña, R.; Perales-Pérez, O.; Román, F.R. Quantum dots of ZnSe(S) doped with copper as nanophotocatalyst in the degradation of organic dyes. *J. Nanosci. Nanotechnol.* **2014**, *14*, 7333–7339. [[CrossRef](#)]
3. Muhammad, F.; Tahir, M.; Zeb, M.; Wahab, F.; Kalasad, M.N.; Khan, D.N.; Karimov, K.S. Cadmium selenide quantum dots: Synthesis, characterization and their humidity and temperature sensing properties with poly-(dioctylfluorene). *Sens. Actuators B Chem.* **2019**, *285*, 504–512. [[CrossRef](#)]
4. Auffan, M.; Rose, J.; Wiesner, M.R.; Bottero, J.-Y. Chemical stability of metallic nanoparticles: A parameter controlling their potential cellular toxicity in vitro. *Environ. Pollut.* **2009**, *157*, 1127–1133. [[CrossRef](#)]
5. Sotomayor, C.G.; Groothof, D.; Vodegel, J.J.; Eisenga, M.F.; Knobbe, T.J.; IJmker, J.; Lammerts, R.G.M.; de Borst, M.H.; Berger, S.P.; Nolte, I.M.; et al. Plasma cadmium is associated with increased risk of long-term kidney graft failure. *Kidney Int.* **2021**, *99*, 1213–1224. [[CrossRef](#)]
6. Abbas, Q.; Yousaf, B.; Amina; Ali, M.U.; Munir, M.A.M.; El-Naggar, A.; Rinklebe, J.; Naushad, M. Transformation pathways and fate of engineered nanoparticles (ENPs) in distinct interactive environmental compartments: A review. *Environ. Int.* **2020**, *138*, 105646. [[CrossRef](#)]
7. Malakar, A.; Kanel, S.R.; Ray, C.; Snow, D.D.; Nadagouda, M.N. Nanomaterials in the environment, human exposure pathway, and health effects: A review. *Sci. Total Environ.* **2021**, *759*, 143470. [[CrossRef](#)]
8. Naito, M.; Yokoyama, T.; Hosokawa, K.; Nogi, K. (Eds.) Chapter 1—Basic Properties and Measuring Methods of Nanoparticles. In *Nanoparticle Technology Handbook*, 3rd ed.; Elsevier: Amsterdam, The Netherlands, 2018; pp. 3–47. ISBN 978-0-444-64110-6.
9. Rivera-Rodriguez, G.; Peralez-Perez, O.; Su, Y.-F.; Alamo-Nole, L. Effect of the Reaction Temperature on the Optical Properties of CdS/Te Quantum Dots Synthesized Under Microwave Irradiation. *MRS Adv.* **2016**, *1*, 2207–2212. [[CrossRef](#)]
10. Sharifi, S.; Behzadi, S.; Laurent, S.; Laird Forrest, M.; Stroeve, P.; Mahmoudi, M. Toxicity of nanomaterials. *Chem. Soc. Rev.* **2012**, *41*, 2323–2343. [[CrossRef](#)]
11. Behzadi, S.; Serpooshan, V.; Tao, W.; Hamaly, M.A.; Alkawareek, M.Y.; Dreaden, E.C.; Brown, D.; Alkilany, A.M.; Farokhzad, O.C.; Mahmoudi, M. Cellular uptake of nanoparticles: Journey inside the cell. *Chem. Soc. Rev.* **2017**, *46*, 4218–4244. [[CrossRef](#)]
12. Demir, E.; Qin, T.; Li, Y.; Zhang, Y.; Guo, X.; Ingle, T.; Yan, J.; Orza, A.I.; Biris, A.S.; Ghorai, S.; et al. Cytotoxicity and genotoxicity of cadmium oxide nanoparticles evaluated using in vitro assays. *Mutat. Res. Toxicol. Environ. Mutagen.* **2020**, *850–851*, 503149. [[CrossRef](#)] [[PubMed](#)]
13. Wang, L.; Chen, S.; Ding, Y.; Zhu, Q.; Zhang, N.; Yu, S. Biofabrication of morphology improved cadmium sulfide nanoparticles using *Shewanella oneidensis* bacterial cells and ionic liquid: For toxicity against brain cancer cell lines. *J. Photochem. Photobiol. B Biol.* **2018**, *178*, 424–427. [[CrossRef](#)] [[PubMed](#)]
14. Kaviyarasu, K.; Kanimozhi, K.; Matinise, N.; Maria Magdalane, C.; Mola, G.T.; Kennedy, J.; Maaza, M. Antiproliferative effects on human lung cell lines A549 activity of cadmium selenide nanoparticles extracted from cytotoxic effects: Investigation of bio-electronic application. *Mater. Sci. Eng. C* **2017**, *76*, 1012–1025. [[CrossRef](#)] [[PubMed](#)]
15. Lovrić, J.; Cho, S.J.; Winnik, F.M.; Maysinger, D. Unmodified cadmium telluride quantum dots induce reactive oxygen species formation leading to multiple organelle damage and cell death. *Chem. Biol.* **2005**, *12*, 1227–1234. [[CrossRef](#)] [[PubMed](#)]
16. Lovrić, J.; Bazzi, H.S.; Cuie, Y.; Fortin, G.R.A.; Winnik, F.M.; Maysinger, D. Differences in subcellular distribution and toxicity of green and red emitting CdTe quantum dots. *J. Mol. Med.* **2005**, *83*, 377–385. [[CrossRef](#)]

17. Luo, Y.-H.; Wu, S.-B.; Wei, Y.-H.; Chen, Y.-C.; Tsai, M.-H.; Ho, C.-C.; Lin, S.-Y.; Yang, C.-S.; Lin, P. Cadmium-Based Quantum Dot Induced Autophagy Formation for Cell Survival via Oxidative Stress. *Chem. Res. Toxicol.* **2013**, *26*, 662–673. [[CrossRef](#)]
18. Omasa, T.; Onitsuka, M.; Kim, W.-D. Cell engineering and cultivation of chinese hamster ovary (CHO) cells. *Curr. Pharm. Biotechnol.* **2010**, *11*, 233–240. [[CrossRef](#)]
19. Donato, M.T.; Tolosa, L.; Gómez-Lechón, M.J. Culture and Functional Characterization of Human Hepatoma HepG2 Cells. *Methods Mol. Biol.* **2015**, *1250*, 77–93. [[CrossRef](#)]
20. Guengerich, F.P. Common and Uncommon Cytochrome P450 Reactions Related to Metabolism and Chemical Toxicity. *Chem. Res. Toxicol.* **2001**, *14*, 611–650. [[CrossRef](#)]
21. Furge, L.L.; Guengerich, F.P. Cytochrome P450 enzymes in drug metabolism and chemical toxicology: An introduction. *Biochem. Mol. Biol. Educ.* **2006**, *34*, 66–74. [[CrossRef](#)]
22. Strober, W. Trypan Blue Exclusion Test of Cell Viability. *Curr. Protoc. Immunol.* **2015**, *111*, A3.B.1–A3.B.3. [[CrossRef](#)] [[PubMed](#)]
23. Derfus, A.M.; Chan, W.C.W.; Bhatia, S.N. Probing the Cytotoxicity of Semiconductor Quantum Dots. *Nano Lett.* **2004**, *4*, 11–18. [[CrossRef](#)]
24. Wang, L.; Nagesha, D.K.; Selvarasah, S.; Dokmeci, M.R.; Carrier, R.L. Toxicity of CdSe nanoparticles in Caco-2 cell cultures. *J. Nanobiotech.* **2008**, *6*, 11. [[CrossRef](#)] [[PubMed](#)]
25. Deng, J.; Gao, C. Recent advances in interactions of designed nanoparticles and cells with respect to cellular uptake, intracellular fate, degradation and cytotoxicity. *Nanotechnology* **2016**, *27*, 412002. [[CrossRef](#)]
26. Shukla, V.; Mishra, S.K.; Pant, H.C. Oxidative stress in neurodegeneration. *Adv. Pharmacol. Sci.* **2011**, *2011*, 572634. [[CrossRef](#)] [[PubMed](#)]
27. Liu, W.; Zhao, H.; Wang, Y.; Jiang, C.; Xia, P.; Gu, J.; Liu, X.; Bian, J.; Yuan, Y.; Liu, Z. Calcium—Calmodulin signaling elicits mitochondrial dysfunction and the release of cytochrome c during cadmium-induced apoptosis in primary osteoblasts. *Toxicol. Lett.* **2014**, *224*, 1–6. [[CrossRef](#)]
28. Messner, B.; Türkcan, A.; Ploner, C.; Laufer, G.; Bernhard, D. Cadmium overkill: Autophagy, apoptosis and necrosis signalling in endothelial cells exposed to cadmium. *Cell. Mol. Life Sci.* **2016**, *73*, 1699–1713. [[CrossRef](#)]
29. Bozcaarmutlu, A. Effect of mercury, cadmium, nickel, chromium and zinc on kinetic properties of NADPH-cytochrome P450 reductase purified from leaping mullet (*Liza saliens*). *Toxicol. Vitro.* **2007**, *21*, 408–416. [[CrossRef](#)]
30. Zhang, L.; Gan, J.; Ke, C.; Liu, X.; Zhao, J.; You, L.; Yu, J.; Wu, H. Identification and expression profile of a new cytochrome P450 isoform (CYP414A1) in the hepatopancreas of *Venerupis (Ruditapes) philippinarum* exposed to benzo[a]pyrene, cadmium and copper. *Environ. Toxicol. Pharmacol.* **2012**, *33*, 85–91. [[CrossRef](#)]
31. Baker, J.R.; Satarug, S.; Edwards, R.J.; Moore, M.R.; Williams, D.J.; Reilly, P.E.B. Potential for early involvement of CYP isoforms in aspects of human cadmium toxicity. *Toxicol. Lett.* **2003**, *137*, 85–93. [[CrossRef](#)]
32. Chen, N.; He, Y.; Su, Y.; Li, X.; Huang, Q.; Wang, H.; Zhang, X.; Tai, R.; Fan, C. The cytotoxicity of cadmium-based quantum dots. *Biomaterials* **2012**, *33*, 1238–1244. [[CrossRef](#)] [[PubMed](#)]

Disclaimer/Publisher's Note: The statements, opinions and data contained in all publications are solely those of the individual author(s) and contributor(s) and not of MDPI and/or the editor(s). MDPI and/or the editor(s) disclaim responsibility for any injury to people or property resulting from any ideas, methods, instructions or products referred to in the content.